VELOCITY DISTRIBUTION MODEL IN OPEN CHANNELS BASED ON THE HARMONIC MEAN DISTANCE

توزيع السرعات فى القنوات المفتوحة اعتمادا على مسافة المتوسط الهرمونى

Saad Moharam; Osami Rageh; Mohsen Ezzeldin; Mahmoud Elgamal; and Mahmoud A. Elashry
Irrigation and Hydraulics Dept, Mansoura university, Faculty of Engineering, Mansoura, Egypt

خلاصة : يقدم البحث طريقة تحليلية جديدة لرسم خطوط كنتور السرعة فى أى قطاع للقنوات المفتوحة اعتمادا على فرضية مسافة المتوسط الهرمونى، وذلك على فرض أن السرعة عند أى نقطة ما فى القطاع تتأثر بخشونة كل نقطة على المحيط وبعدها منها. تم إنشاء برنامج كمبيوتر لحساب متوسط المسافة الهرمونية لكل النقاط داخل أى قطاع للقنوات المفتوحة آخذا فى الاعتبار تأثير السطح الحر للمياه والخشونة المركبة. اعتمادا على المتوسط الهرمونى للمسافة يتم التنبؤ بتوزيع السرعات باستخدام قانون التوزيع الأسى وقانون التوزيع اللوغاريتمى للسرعة. تم حساب معاملات السرعة (α و β)، ومكان أقصى سرعة، والنسبة بين أعلى سرعة للسرعة المتوسطة (u_{max} / V). النموذج المقدم تم تحقيقه مع منحنيات سرعة مقاسة لقطاعات مستطيلة من عمل سابق لباحثين آخرين وأعطى موافقة جيدة.

ABSTRACT:

A new analytical technique for drawing isovel patterns in any open channel cross section is presented based on the Harmonic Mean Distance concept. It is assumed that the instantaneous velocity at a point in the section is affected by the roughness of each point in the boundary and its distance from it. A computer program is established to compute the Harmonic Mean Distance at all points for open channel of different cross sections, taking into consideration the effect of the free surface and the composite roughness. Based on the Harmonic Mean Distance the 2-D velocity distribution is predicted using the power law distribution and the logarithmic distribution. Also the velocity factors (α and β), the location of the maximum velocity, and the ratio of the maximum to the mean velocity (u_{max} / V) are calculated. The proposed model is verified with measured velocity profiles from a previous work of other researchers on rectangular cross sections and showed good agreement.

1-INTRODUCTION

Predicting the velocity distribution solves various problems in open channel hydraulics. The most important of which is estimating precisely the discharge which is the most significant task in water resources management. Close to this the estimation of the energy and the momentum correction coefficients, and the estimation of the sheer stress distribution which is the main factor affects the distribution of sediment concentration. The isovel patterns in an open channel cross section are affected by several uncertain factors, among these the boundary roughness, the cross section geometry, the channel alignment, the presence of bends, the properties of the flowing water, the type of flow, the flow regimes, and the obvious effect of the free surface.

Several studies have been carried out to investigate the velocity profile for many years. Some investigators have solved equations combined with turbulent models (Sofialidis and Prinos 1998; Bonakdari, et al 2008). Chiu(1987-1989) proposed a new approach to the problem based on a probability concept which later was followed by related studies, Chiu and Hsu (2006). Maghrebi and Ball (2006) presented a new technique using the similarities between the magnetic field and the isovel contours. Most of the models worked in these studies did not deal with the effect of the free surface as a variable. While in this study the effect of the free surface provides a degree of freedom that can be later calibrated experimentally.

In this study a new technique is presented to simulate the isovels based on the Harmonic Mean Distance (HMD). This new term is first defined by Fukushi (2006). In a hydraulic cross section the HMD has a small value near the boundary and increases as getting far of it. The HMD distribution simulates the velocity distribution in an obvious way.

2-THE HARMONIC MEAN DISTANCE

In an arbitrary hydraulic cross section, Fukushi (2006) defined the Harmonic Mean Distance of a point inside the section as: The harmonic mean of

Accepted June 30, 2010.

the distances between the point and the boundary, Fig. 1.

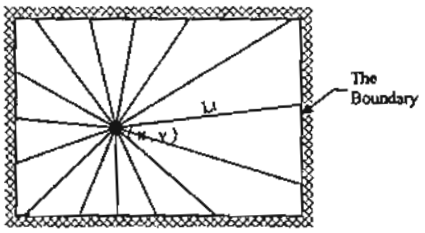

Fig. 1. The concept of the Harmonic Mean Distance

The Harmonic Mean Distance can be calculated from the equation (after Fukushi, 2006).

$$\frac{N}{HMD(x,y)} = \sum_{i=1}^{N} \frac{1}{L_i(x,y)} \tag{1}$$

and for $N = \infty$

$$\frac{2\pi}{HMD(x,y)} = \int_0^{2\pi} \frac{1}{L(x,y)} d\theta \tag{2}$$

in which N is the number of rays emitted from point (x, y) and L_i is the distance between point (x, y) and the boundary on the ray designated by index i.

Fukushi (2006) introduced the free surface as a kind of weak wall with smaller roughness, Fig. 2. For the rays that intersect with the free surface, the distances L_j are multiplied with a factor F_s in order to weaken their weights. Eq. (1) becomes

$$\frac{N}{HMD(x,y)} = \sum_{i=1}^{N_1} \frac{1}{L_i(x,y)} + \sum_{j=1}^{N_2} \frac{1}{L_j(x,y)F_s} \tag{3}$$

where L_j is the distance between point (x, y) and the free surface on the ray designated by index j. N_1 and N_2 are the number of rays in the region (A_1) and (A_2) respectively. F_s is the free surface weight factor. When F_s is equal to 1 the free surface is equal to the rest of the boundary in roughness. When F_s is larger than 1 the free surface is less than the rest of the boundary in roughness, and the larger F_s the weaker the free surface. When F_s has a large value or tends to infinity the effect of the free surface is neglected.

Although the free surface is much less in roughness than the rest of the boundary, its roughness is considered a degree of freedom in the proposed model.

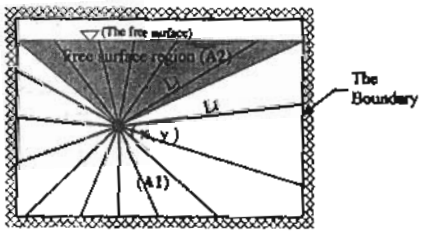

Fig. 2. Introducing the free surface to the Harmonic Mean Distance concept

for $N = \infty$ Eq. (3) becomes

$$\frac{2\pi}{HMD(x,y)} = \int_{A_1} \frac{1}{L(x,y)} d\theta + \int_{A_2} \frac{1}{L(x,y)F_s} d\theta \tag{4}$$

Other new concept is the Harmonic Hydraulic Radius (HHR) given by (Fukushi 2006) as a new definition of the usual hydraulic radius. The HHR is the arithmetic mean of the HMDs.

$$HHR = \frac{\sum_{i=1}^{M} HMD_i}{M} \tag{5}$$

The Hydraulic cross section is meshed and M is the number of points in the section. Fukushi (2006) concentrated his study on this term. He used the Harmonic Hydraulic Radius instead of the usually known Hydraulic Radius in the standard Manning equation.

$$V = \frac{1}{n} HHR^{(2/3)} S^{(1/2)} \tag{6}$$

where V is the average velocity, n is the Manning coefficient, and S is the slope. The hydraulic radius $(R = A / P)$ can be determined in a model by multiplying the prototype radius by the model length ratio L_r, and so is the Harmonic Hydraulic Radius. Both are dependent on the similarity ratio. Other important term is the ratio between the HHR and the hydraulic radius, C_h.

$$C_h = \frac{R}{HHR} \tag{7}$$

In circular section at full flow R = 0.5 unit length, HHR = 0.557 unit length analytically calculated, and C_h = 0.89. Fukushi(2006) applied Eq. (6) on sewer pipes and deduced new Hydraulic Elements charts for partially full pipe flow which had agreed with several recorded data on sewer pipes.

3-DEVELOPING THE HARMONIC MEAN DISTANCE EQUATION

In this paper the HMD equation is modified in order to introduce the composite roughness. The roughness of each individual segment in the boundary is indicated by a coefficient $(s_f)_j$ that is inversely proportional to the surface roughness, Fig. 3. This means that the small value of s_f indicates a rougher segment of the boundary. s_f for the free surface is F_s. The HMD equation becomes:

$$\frac{N}{HMD(x,y)} = \sum_{j=1}^{j=k}\left[\sum_{i=1}^{i=N_j}\frac{1}{L_i(x,y)(s_f)_j}\right] \tag{8}$$

when $N = \infty$ Eq. (8) becomes

$$\frac{2\pi}{HMD(x,y)} = \sum_{j=1}^{j=k}\int_{A=j}\frac{1}{L(x,y)(s_f)_j}d\theta \tag{9}$$

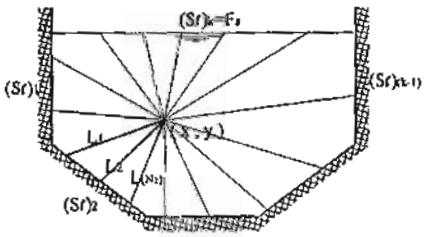

Fig. 3. Introducing the composite roughness to the HMD concept

S_f is the smoothness factor, k is the number of segments in the boundary including the free surface, and N_j is the number of rays that directly intersect with segment designated by index j.

The Harmonic Mean Distance has small values near the boundary increasing as getting far from it. The distribution of the HMD is non linear and the point of Maximum HMD is closer to the segments that has less roughness. Which means that the HMD distribution simulates the velocity distribution in a way that evaluates all distances from a point to the boundary. If a point lies very close to the boundary its HMD tends to zero. For a point on the boundary the HMD can not be calculated because L_i must not be zero, and so the HMD can be calculated for all points inside the section. Figs. 4, and 5 are an illustrative example that shows the distribution of HMD in a trapezoidal cross section with a free surface weight factor, F_s = 3.

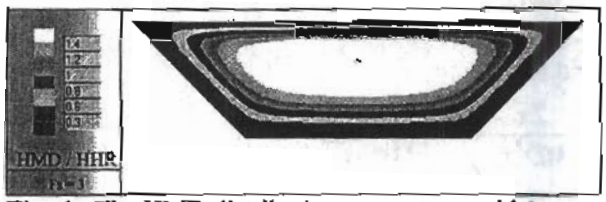

Fig. 4. The HMD distribution over a trapezoidal cross section

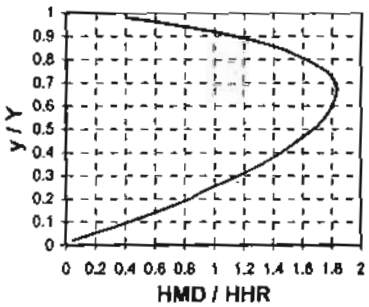

Fig. 5. The vertical HMD distribution at the center (cross section in Fig. 4), where Y is the total depth, and y is the distance from bed.

The advantage of the harmonic mean is that it gives larger weights to the shortest distances, this agrees with the fact that the closer wall has great effect on the velocity at a point than the further one. This effect can be controlled by raising the denominators of both sides of Eq. (8) to a power C_f,

which makes Eq. (8) becomes:

$$\frac{N}{\left[HMD(x,y)\right]^{F_f}} = \sum_{j=1}^{j=k}\left[\sum_{i=1}^{i=N_j}\frac{1}{\left[L_i(x,y)(s_f)_j\right]^{F_f}}\right] \qquad (10)$$

in which C_f is the contour factor, the contour lines of the HMD can be controlled depending on the value of C_f. If C_f is larger than 1, the weight of the short distances gets larger, the contour lines become more parallel to the walls, and the maximum HMD occurs closer to the weak walls. On the other hand if C_f is smaller than 1, the short distances lose some of their weights, and the maximum HMD occurs closer to the center of the section. C_f is another degree of freedom. Figures 6, and 7 show the HMD distribution over a square section with the variation of C_f. F_s is taken equal to 6.0.

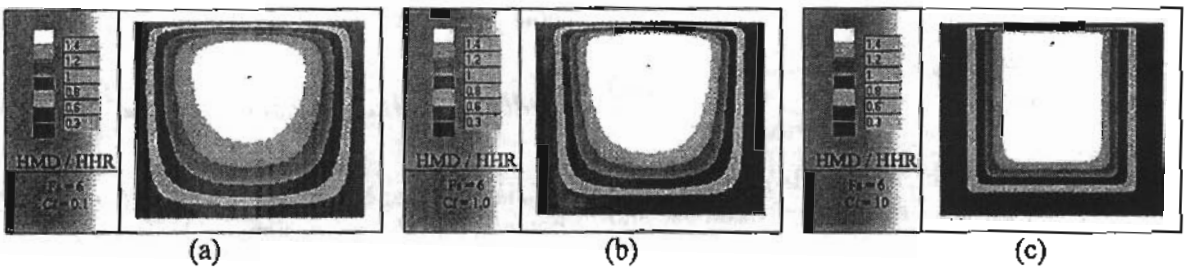

(a) (b) (c)

Fig. 6. The HMD distribution over a square cross section: (a) C_f=0.1; (b) C_f=1.0; (c) C_f=10

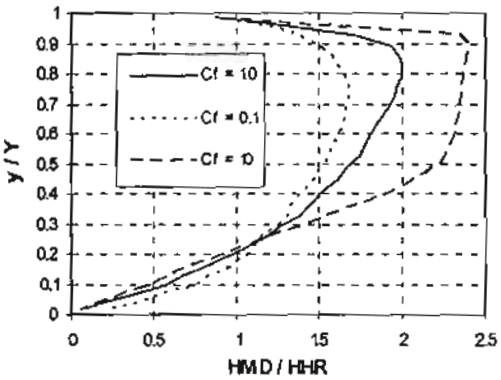

Fig. 7. The vertical HMD distribution at the center line (cross section in Fig. 6.)

4-VELOCITY DISTRIBUTION

The turbulent velocity distribution in a pipe cross section or in an open channel cross section is given by one of two equations, the Power law distribution, Eq. (11), and the Universal Prandtl Von-Karman Logarithmic distribution, Eq. (12).

$$u = u_* C_1 \left(\frac{L}{K}\right)^{\frac{1}{m_1}} \qquad (11)$$

$$u = u_* C_2 \log\left(\frac{L}{L_o}\right) \qquad (12)$$

in which, u is the instantaneous velocity; C_1 and C_2 are constants; L is the valid length from the point to the boundary; L_o is the constant of integration in the logarithmic law; K is the physical roughness mean height; u_* is the sheer velocity $u_* = \sqrt{\tau_o / \rho}$, where τ_o is the average boundary sheer stress and ρ is the mass density; and m_1 is the denominator of exponent of the power law distribution.

In the power law distribution, Eq. (11), the value of the exponent denominator m_1 depends on the degree of turbulence, it varies between 4 and 12, m_1 = 7 is in agreement with large number of experimental measurements of turbulent velocity profiles (Chen 1991). m_1 = 2 gives a parabolic laminar distribution.

In the logarithmic distribution Eq. (12), when the surface is rough, the constant L_o depend on the roughness height K,

$$L_o = m_2 K \tag{13}$$

the value of the constant m_2 is estimated by 1/30 driven from Nikuradse's experimental data on rough pipes. sand grains were cemented to the inner walls of pipes to fabricate an artificial roughness. The Logarithmic distribution for rough surfaces becomes, (after Chow, 1959):

$$u = u_* C_2 \log\left(\frac{L}{m_2 K}\right) \tag{14}$$

The roughness height in Eq. (14) is the mean diameter of the sand grains used by Nikuradse and is Known as the Nikuradse sand roughness. When the surface is smooth, L_o depends on the laminar-sub layer.

$$L_o = \frac{m_2 \upsilon}{u_*} \tag{15}$$

where υ is the kinematic viscosity, the constant, m_2, is estimated by 1/9 also by Nikuradse. The logarithmic distribution for smooth surfaces becomes:

$$u = u_* C_2 \log\left(\frac{L u_*}{m_2 \upsilon}\right) \tag{16}$$

From Eqs. (13) and (15) the value of the roughness height for smooth surfaces can be replaced leaning on Nikuradse's results,

$$K = \frac{30\upsilon}{9u_*} \tag{17}$$

this replacement is useful while introducing data to the model, and this in order to use Eqs. (11) and (14) in both rough and smooth cases.

The proposed model uses Eq. (10) to calculate the HMD taking into consideration the roughness of the boundary and the effect of the free surface in calculating the Harmonic Mean Distance. Also Eq. (10) includes a new calibrating parameter, C_f, which added flexibility to it. In this paper a theoretical relation between the HMD and the velocity is introduced. Consider a constant length X that makes:

$$\frac{HMD(x,y)}{X} = \frac{L}{K} \tag{18}$$

L is the valid length from the point (x , y) to the boundary; and K is the valid roughness.

$$HMD(x,y) = HarmonicMean(L_i . s_{f_i}) = \frac{L.X}{K} \tag{19}$$

L_i is the distance between the point (x , y) and the boundary on the ray designated by index i ; and s_{fi} is the smoothness factor of the intersecting segment on the boundary with the ray designated by i. The smoothness factor, $s_{f\,i}$, is assumed to be inversely proportional to the local roughness, K_i. Consider a length X` as a constant of variation.

$$s_{f_i} = \frac{X`}{K_i} \tag{20}$$

the HMD equation becomes

$$HMD(x,y) = HM\left(\frac{L_i . X`}{K_i}\right) \tag{21}$$

X` can be taken as a common factor

$$HMD(x,y) = X`.HM\left(\frac{L_i}{K_i}\right) \tag{22}$$

substituting Eqs. (19) and (22) in the velocity distribution Eqs. (11) and (14) lead to Eqs. (23) and (24).

$$u = u_* C_1 \left(\frac{X` . HM(\frac{L_i}{K_i})}{X} \right)^{\frac{1}{m_1}} \quad (23)$$

$$u = u_* C_2 \log \left(\frac{X` . HM(\frac{L_i}{K_i})}{m_2 . X} \right) \quad (24)$$

The values of X and $X`$ are unknowns and are to be eliminated. In Eq. (23) $m_1$ is replaced by $m_1`$ because the HMD distribution is non-linear and C_1 is replaced by $C_1`$ eliminating $(X` / X)^{1/m1`}$, Eq. (25). In Eq. (24) $m_2$ is replaced by $m_2`$ to eliminate $(X` / X)$, Eq. (26).

$$u = u_* C_1 \left(HM(\frac{L_i}{K_i}) \right)^{\frac{1}{m`_1}} \quad (25)$$

$$u = u_* C_2 \log \left(\frac{HM(\frac{L_i}{K_i})}{m`_2} \right) \quad (26)$$

Although $m_1`$ and $m_2`$ are expected to be near the range of previous works they provides one degree of freedom that should be calibrated. The Power law distribution represented in Eq. (25) is more sensitive in analysis than the Logarithmic distribution represented in Eq. (26). The reason is that the value of $m_1`$ affects the curvature of the power law distribution more than the effect of $m_2`$ on the curvature of the Logarithmic distribution, i.e. the Logarithmic distribution is more stiff somehow. Eq. (26) might need a mathematical modification, but this will not take place presently in this study. Figures 8 and 9 show the effect of changing the value of $m_1`$ and $m_2`$ on the velocity distribution for a rectangular cross section with constant conditions.

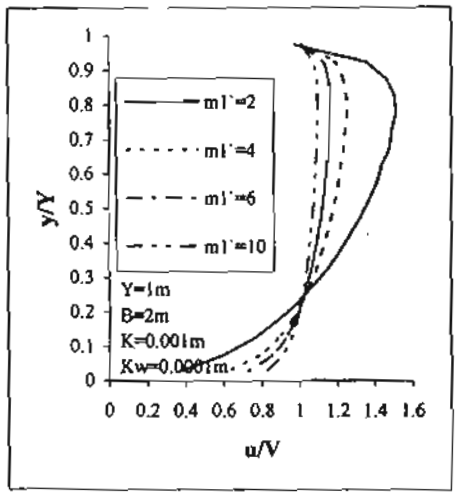

Fig. 8. The effect of changing $m_1`$ on the vertical power-law velocity distribution at the centerline of a rectangular cross section.

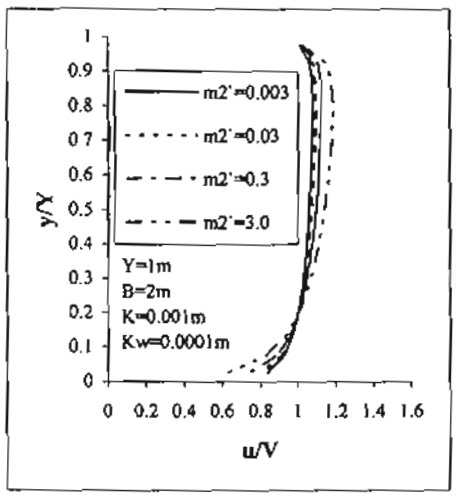

Fig. 9. The effect of changing $m_2`$ on the vertical logarithmic velocity distribution at the centerline of a rectangular cross section.

The velocity profile is normalized by dividing the velocity of all points by the average velocity V. the sheer velocity, u_*, the constants, $C_1`$, and C_2 are then not important because the normalized velocity profile will remain unchanged. Some researchers have behaved this way (Maghrebi and Ball 2006; Sofialidis and Prinos 1998). Eqs (25) and (26) are used in the model to predict the velocity distribution after normalization. The HMD also should be normalized especially when

introducing the smoothness factor, s_f, using the surface roughness, K, as in Eq. (20), because the value of $X`$ is unknown. The point of maximum HMD is that of the maximum velocity. Figures 10, 11, and 12 are examples that show the distribution of the HMD, and the distribution of velocity using Eqs. (25) and (26). K_w is the free surface roughness, and is introduced in the following example by 0.00005 m equals to 1/20 of the surface roughness of the rest of the boundary.

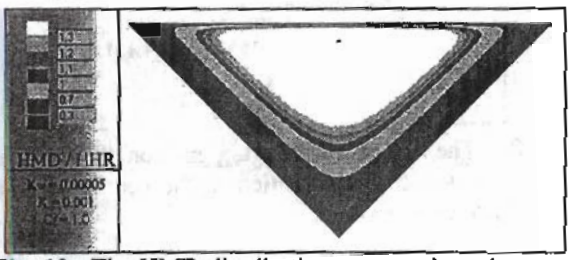

Fig. 10. The HMD distribution over a triangular cross section.

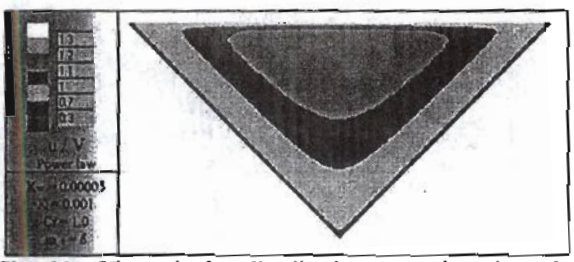

Fig. 11. The velocity distribution over the triangular cross section in Fig. 10. based on the power law in Eq. (25).

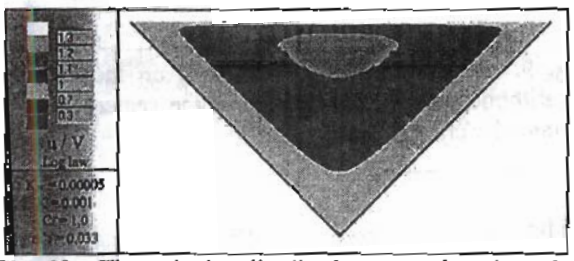

Fig. 12. The velocity distribution over the triangular cross section in Fig. 10. based on the logarithmic law in Eq. (26).

5-MODEL VERIFICATION AND RESULTS

The experimentally measured data of the velocity profiles chosen to verify the model is taken from Maghrebi and Ball (2006). The flume cross section was rectangular of 0.25m wide, and 0.29m high with smooth boundary. The experiments were carried out for three flow depths of 0.15m, 0.2m, 0.25m, corresponding to B/Y of 1.67, 1.25, 1.0, respectively. Where B is the width of the section, and Y is the total depth. The velocity profiles were measured at the center line vertically using a miniature propeller with a diameter of 1cm. The surface roughness, K, is introduced reasonably by 0.001m, noted that Eq. (17) requires the energy slope which is not mentioned in the given data. The proposed model has three degrees of freedom that are still not calibrated:

1- The free surface roughness, K_w, is introduced by 1/20 of K.
2- The contour factor, C_f, is introduced by 1.0
3- $m_1`$ is introduced by 6.0, and $m_2`$ is introduced by 0.1

A comparison between the measured velocity profiles and the computed velocity profiles using the proposed model is shown in Fig. 13. The reduction of the velocity near the water surface that appears in the profile computed by the proposed model can be controlled by adjusting the value of K_w. The maximum velocity computed by the model is below the free surface even when the channel is wide. Seckin (2005) showed that u_{max} occurred below the water surface for all his test cases. The proposed model gives a very good simulation of the velocity near the boundary. The flume used by Maghrebi and Ball (2006) was 8.0m long and the location of the tested section is 5.5m from the upstream entrance. The development of the velocity profile is not checked out, and that might explain why the maximum measured velocity in the first two cases occurs in the lower half of the depth. However, the measured velocity profiles are accepted in more than one paper.

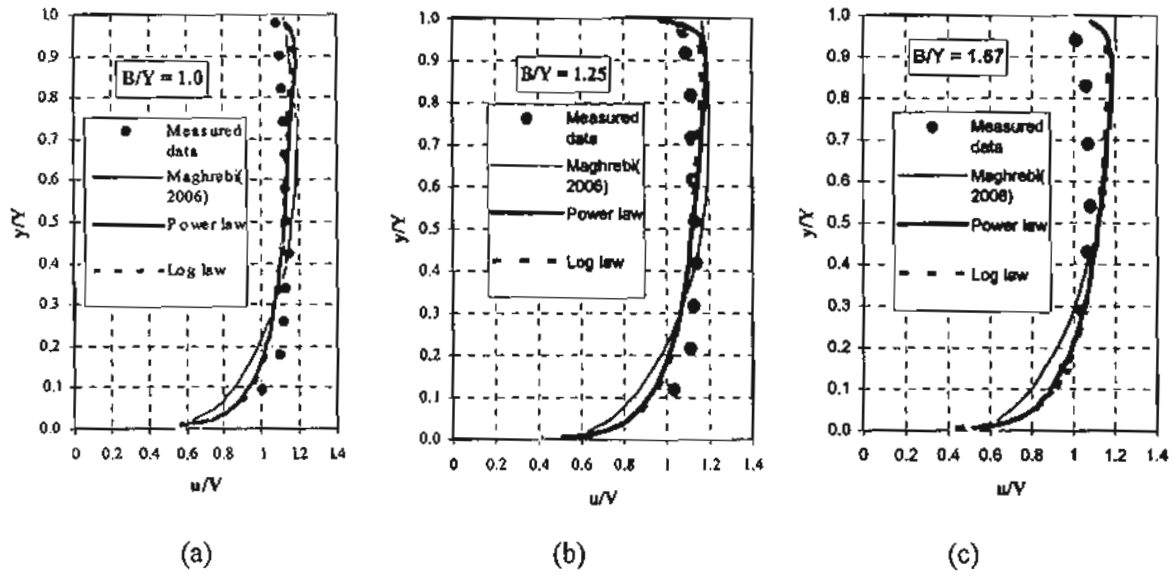

Fig. 13. Comparison of measured velocity profiles along center line of flume flow with profile of proposed model: (a) $B/Y = 1.0$; (b) $B/Y = 1.25$; (c) $B/Y = 1.67$

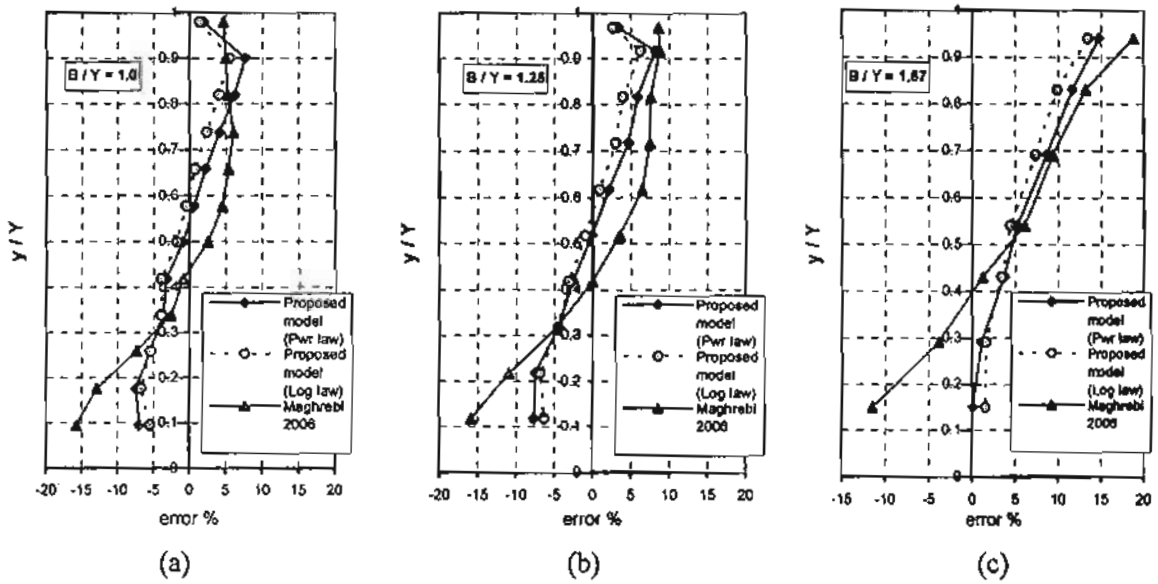

Fig. 14. Percentage of error in velocity profile along center line of flume flow: (a) $B/Y = 1.0$; (b) $B/Y = 1.25$; (c) $B/Y = 1.67$, [error = (calculated – measured) / measured]

The percentage of error between the computed and measured velocity profile is calculated, Fig. 14. The error in the proposed model is less than the error in the model proposed by Maghrebi (2006).

The isovel contours for the three cases of B/Y are shown in figures 15, 16, and 17. The point of the maximum velocity is the same for both the power

and the logarithmic distribution in each case, because it depends on the maximum HMD. The isovels shows a near equivalence of the power and the logarithmic distributions. A number of investigators (Brownlie 1983;Wright and Parker 2004) have shown the similarity between the logarithmic velocity distribution and the one-sixth power distribution. Although the composite roughness can be easily introduced to the model, the roughness of all segments of the boundary is introduced here by the same value.

(a) (b)

Fig. 15. Isovel contours by the proposed model for $B/Y = 1.0$: (a) Power distribution; (b) Logarithmic distribution.

(a) (b)

Fig. 16. Isovel contours by the proposed model for $B/Y = 1.25$: (a) Power distribution; (b) Logarithmic distribution.

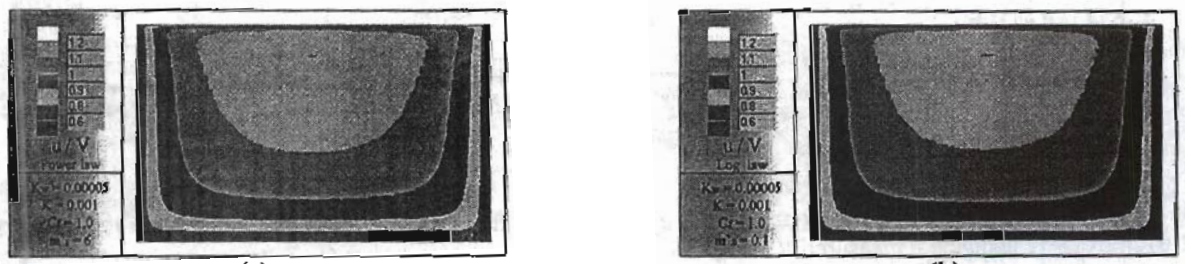

(a) (b)

Fig. 17. Isovel contours by the proposed model for $B/Y = 1.67$: (a) Power distribution; (b) Logarithmic distribution.

6- VELOCITY FACTORS

The velocity factors are not affected by the normalization. Since the normalized velocity is calculated for all points produced by meshing the cross section, the kinematic energy correction factor, α, and the momentum correction factor, β, can be calculated by:

$$\alpha = \frac{\sum (\frac{u_i}{V})^3 a}{(\frac{V}{V})^3 A} = \frac{\sum u_i^3 a}{V^3 A} \quad (27)$$

$$\beta = \frac{\sum (\frac{u_i}{V})^2 a}{(\frac{V}{V})^2 A} = \frac{\sum u_i^2 a}{V^2 A} \quad (28)$$

where A is the cross section area, and a is the area of the individual mesh element. The values of α and β are very significant in the case of the compound sections. Because of the complexity in computing the velocity correction factors, they are assumed equal to unity in most of hydraulic calculations. In turbulent flow in regular channels α and β rarely exceeds 1.15 and 1.05, respectively, (Henderson 1966).

The ratio of the maximum to the mean velocity (u_{max} / V) is related to the velocity factors. Fig. 18 shows the variations of α, β, and (u_{max} / V) for the proposed model with the ratio B/Y. The values of α, β, and (u_{max} / V) are lower in the wider section, this might be due to the reduction in the effect of sides on the velocity distribution.

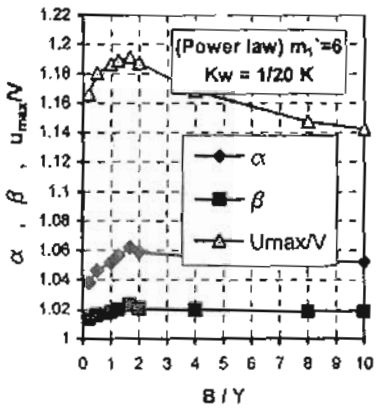

Fig. 18. The variation of α, β, and (u_{max} / V) calculated by the proposed model with B/Y (Power law).

7-CONCLUSIONS

A theoretical approach of the relation between the Harmonic Mean Distance and the velocity is presented. Based on the HMD, a new analytical technique for drawing the dimensionless isovel contours for any open channel cross section is proposed. The model takes into consideration the composite roughness, the section geometry, and the effect of the free surface. The model is based on a simple idea but is engaged with three calibrating parameters:

1- The free surface roughness K_w.
2- The contour factor C_f.
3- the constants m_1` and $m_2$`.

The model was verified with measured velocity profiles from a previous work by other researchers on rectangular cross sections, and showed good agreement.

The major advantage of the proposed model is that it can deal with the free surface effect as a degree of freedom that might be calibrated in a future work.

REFERENCES:

1- Bonakdari, H., Larrarte, F., Lassabatere, L., and Joannis, C. (2008). "Turbulent velocity profile in fully-developed open channel flows." Environ Fluid Mech 8:1–17.

2- Brownlie, W. (1983). "Flow depth in sand bed channels." J. Hydr. Eng., ASCE. 109(7), 959-990.

3- Chen, C. L. (1991) "Power law of flow resistance in open channel: Manning formula revisited." Centennial of Manning's formula, Water Research, Charlottesville, Va.,206-240.

4- Chow, V. T. (1959). Open-channel hydraulics, McGraw-Hill, New York.

5- Chiu, C. L., and Hsu, S. M. (2006). "Probabilistic approach to modeling of velocity distributions in fluid flows." J. Hydrology 316(2006) 28–42.

6- Chiu, C. L. (1987). "Entropy and Probability concepts in hydraulics." J. Hydr. Eng., ASCE. 113(5), 583-600.

7- Chiu, C. L. (1989). "Velocity distribution in open channel flow." J. Hydr. Eng., ASCE. 115(5), 576-594.

8- Henderson, F. M. (1966). Open channel Flow, Macmillan, New York.

9- Fukuchi, T. (2006). "Hydraulic elements chart for pipe flow using new definition of hydraulic radius." J. Hydr. Eng., ASCE. 132(9), 990-994.

10- Maghrebi, M. F., and Ball, J. E. (2006). "New method of estimating disharge." J. Hydr. Eng., ASCE. 132(10), 1044-1051.
11- Seckin, G. (2005) "Maximum and mean velocity relationships in laboratory flumes with different cross-sectional shapes." J. Civ. Eng. 32: 413-419.
12- Sofialidis, D., and Prinos, P. (1998). "Compound open-channel flow modeling with nonlinear low-Reynolds k-ε models." J. Hydr. Eng., ASCE. 124(3), 253-262.
13- Wright, S., and Parker, G. (2004) "Density stratification effects in sandbed rivers." J. Hydr. Eng., ASCE. 130(8), 783-795.

NOMENCLATURE

The following symbols are used in this paper:

A	Cross section area;
A_1	Region at which rays intersect with the wetted perimeter;
A_2	Region at which rays intersect with the free surface;
a	Area of individual mesh element;
B	Open-channel width;
C_1, C_1`, C_2	Constants;
C_f	Contour factor;
C_h	Ratio between the Harmonic hydraulic Radius and the hydraulic radius;
$d\theta$	Radian element;
F_s	Free surface weight factor;
HM	Harmonic Mean
HMD	Harmonic Mean Distance;
HHR	Harmonic Hydraulic Radius;
i, j, k	Indices;
K	Physical roughness mean hight;
K_w	Free surface roughness
L	Length from the point to the boundary;
L_o	Constant of integration in the logarithmic distribution;
L_r	Length ratio;
M	Number of points in the section after meshing;
m_1	Denominator in exponent in power velocity distribution;
m_2	Constant of variation between the roughness height and the constant of integration in the logarithmic velocity distribution;
m_1`	Denominator in exponent in power velocity distribution after applying the harmonic mean;
m_2`	Constant in the logarithmic velocity distribution after applying the harmonic mean;
N	Total number of rays emitted from a point in the cross section;
N_1	Number of rays emitted from a point to the wetted perimeter;
N_2	Number of rays emitted from a point to the free surface;
n	Manning`s roughness coefficient;
P	Wetted perimeter;
R	Hydraulic radius;
S	Longitudinal channel slope;
s_f	Smoothness factor;
u	Instantaneous streamwise velocity;
u_*	Sheer velocity;
u_{max}	Maximum streamwise velocity;
V	Average streamwise velocity;
x	Horizontal coordinate perpendicular to the direction of flow;
X, X`	Constants;
y	Vertical coordinate with zero at the cross section bed;
Y	Total water depth;
α	Kinematic energy correction factor;
β	Momentum correction factor;
υ	Kinematic viscosity;
ρ	Water density; and
τ_o	Average boundary shear stress